Computer-Aided Segmentation and Estimation of Indices in Brain CT Scans

Adnan Qureshi
adnan.qureshi@beds.ac.uk
Vitaly Schetinin
vitaly.schetinin@beds.ac.uk

Institute for Research in Applicable Computing
University of Bedfordshire
Luton, UK.

Abstract

The importance of neuro-imaging as one of the biomarkers for diagnosis and prognosis of pathologies and traumatic cases is well established. Doctors routinely perform linear measurements on neuro-images to ascertain severity and extent of the pathology or trauma from significant anatomical changes. However, it is a tedious and time consuming process and manually assessing and reporting on large volume of data is fraught with errors and variation. In this paper we present a novel technique for segmentation of significant anatomical landmarks using artificial neural networks and estimation of various ratios and indices performed on brain CT scans. The proposed method is efficient and robust in detecting and measuring sizes of anatomical structures on noncontrast CT scans and has been evaluated on images from subjects with ages between 5 to 85 years. Results show that our method has average ICC of ≥ 0.97 and, hence, can be used in processing data for further use in research and clinical environment.

1 Overview and problem statement

Linear measurements on axial CT scans provide clinicians and surgeons opportunity to ascertain differential diagnoses of neuropsychiatric disorders, outcomes of clinical and surgical interventions, geriatric changes and deleterious effects of drugs. Quantitative assessment of neuro-images is an effective approach to reveal structural changes in conditions such as Alzheimer's disease (AD), Schizophrenia, Huntington's disease, hydrocephalus and many other neurological and psychiatric disorders [1, 2, 11, 12]. The typical measurements performed on the axial CT scans (fig. 1a, details in table 1) are used to estimate indices and ratios such as Evan's Ratio (ER), Bifrontal Index (BFI), Bicaudate Index (BCI), Cella Media Index (CMI), Frontal Horn Index (FHI), Ventricular index (VI), Huckman number (HN) and 3rd ventricle width (V3) [3]. Manual measurements of regions of interest (ROI) are still considered 'gold standard', however, these are time consuming and a robust and efficient method is required to assist the researchers and to our knowledge, there is no automated system for performing measurements and calculation of these from CT scans.

Computer aided quantitative radiology and volumetry studies of the human anatomy and pathology have been undertaken by many researchers and a surfeit of image segmentation methods have been proposed [10]. However, in medical images an ROI can have dissimilarity of pixel intensity, inhomogeniety of background contribution and noise, and spatially

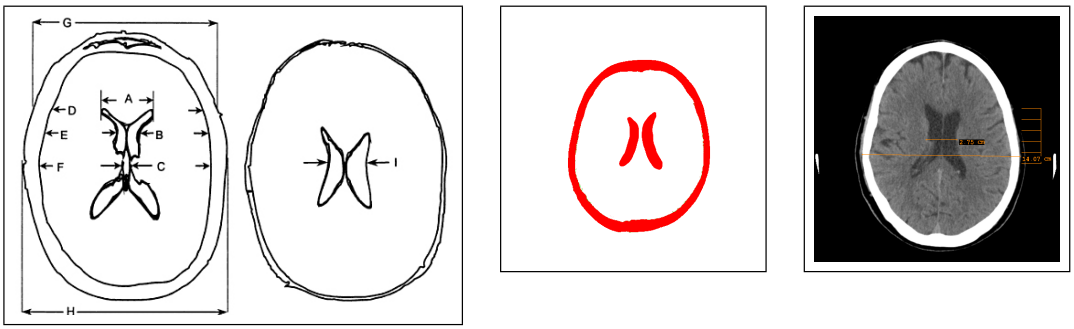

(a) (b) (c)

Figure 1: Measurements on Axial CT Scans (a) and Manual Labelling (b, c).

blind methods in these cases can result in disjoint, quasi-homogeneous regions [9]. To preserve the spatial relationship between the pixels and neighbourhood information, spatially guided techniques such as region growing and merging, active contours and level sets show better results [10].

The extensive and tenable integration of computational intelligence in medical problems can be attributed to the fact that these systems can adaptively learn and optimize the relationship between inputs and outputs [4, 5, 6, 7, 8]. Medical images e.g., CT scans, usually have inhomogeniety of background and noise; and recognition of ROI in images with similar characteristics using ANN can give plausible results [13]. In addition, ANN's can be trained using a few images which have been manually annotated and labelled in order to learn to recognize the ROI.

2 Methodology

The proposed methodology uses ANN to segment the input images into ROI. Measurements of landmark regions are then used for calculating the various ratios and indices. The input images are DICOM (Digital Imaging and Communications in Medicine) files and the training set has been manually segmented and measured by radiology experts (Figure 1b, 1c). The dataset used for training, validation and testing consists of noncontrast CT studies from different subjects. The studies include subjects of both genders and between ages 5 to 85 years. Our method is used on axial CT slices.

2.1 Correction of Orientation of Head

The first step is to align the head into proper orientation on the CT image to ensure that the reference points for measurements are properly identified. This is done by demarcating the bony protuberance of the anterior and posterior falx cerebri attachments as these landmarks are usually not affected in traumatic and pathological cases in which the brain tissue may show abnormalities. The skull boundaries are extracted using Canny edge detection with $\sigma = 2$ and $threshold = 0.5$ in our experiments, and properties of connected regions are measured. Then the curve of the skull bone is modelled as a function of the location and height of pixels and the extrema represent the protuberances which are used to find any shift P_{shift} in the orientation.

(a) (b) (c)

Figure 2: Correction of orientation of CT Scans.

Taking *arctan* of the P_{shift} with reference to the skull centroid calculated earlier, gives the rotation angle θ° to be corrected (Figure 2). An ideal midline can also be drawn using skull centroid which, in normal cases, would pass through the septum pellucidum. Identifying the septum pellucidum and its location with reference to skull can be used for measuring the midline shift which is an important clinical feature in assessment of traumatic or pathological conditions.

2.2 Detection of Candidates for Measurements

An input image is represented as an $(n \times m)$ matrix $X = \{x_{ij}\}, i = 1 \ldots n, j = 1 \ldots m$, whose pixels can either belong to a region of interest class Ω_0 or to a non region Ω_1. A function $u_{ij} = \phi(X; i, j)$ reflects the brightness of the pixel x_{ij} influenced constantly or variably by the neighbourhood. The function is estimated in a rectangular window P, which is a $(k \times k)$ matrix containing the central pixel x_{ij} and $r-1$ nearest pixels, where $r = k^2$. Then by sliding the window P through the image X, every central pixel x_{ij} can be assigned to one of the two classes Ω_0 or Ω_1. The sliding window transforms the image X into an $r \times q$ matrix Z where $q = (n-k+1)(m-k+1)$ and the central element of a vector $z \in Z$, hence, represents the pixel x_{ij} of the input image. The matrix Z is fed to the ANN with one hidden layer and the output neuron makes a decision $y_c = \{0,1\}, c = 1 \ldots q$, on the central element of cth column vector $z^{(c)}$, thus, classifying the image pixels to classes Ω_0 or Ω_1 as proposed by [13]. The ANN is trained with standard back propagation technique aiming to minimize an error function ε for a given number of training epochs. We use images whose pixels are manually labelled and assigned either to class Ω_0 or Ω_1 by a radiology expert Fig. 3b and the ANN is trained (Fig. 3c) to approximate these. The approach is implemented to identify both ventricles and skull as ROI for subsequent measurements and estimations of indices.

The output from the neural network classifies pixels of the input image into ROI as shown in Fig. 3e. In this binarized image, the discontinuities within the regions and the non-smooth boundaries are further refined using active contours using output of ANN for automatic seeding. The values of curve length μ and curvature κ are empirically estimated in our experiments to ensure a good approximation of the edges of regions. This step generates a binary image as output with the skull and ventricles' boundaries clearly demarcated as in Fig. 3f and 3g respectively.

2.3 Measurements and Estimation of Indices

The CT scan studies are viewed using 'brain window' (width = 80, length = 40) with image size of 512×512 pixels and a reference ruler is overlaid on the images to calibrate our

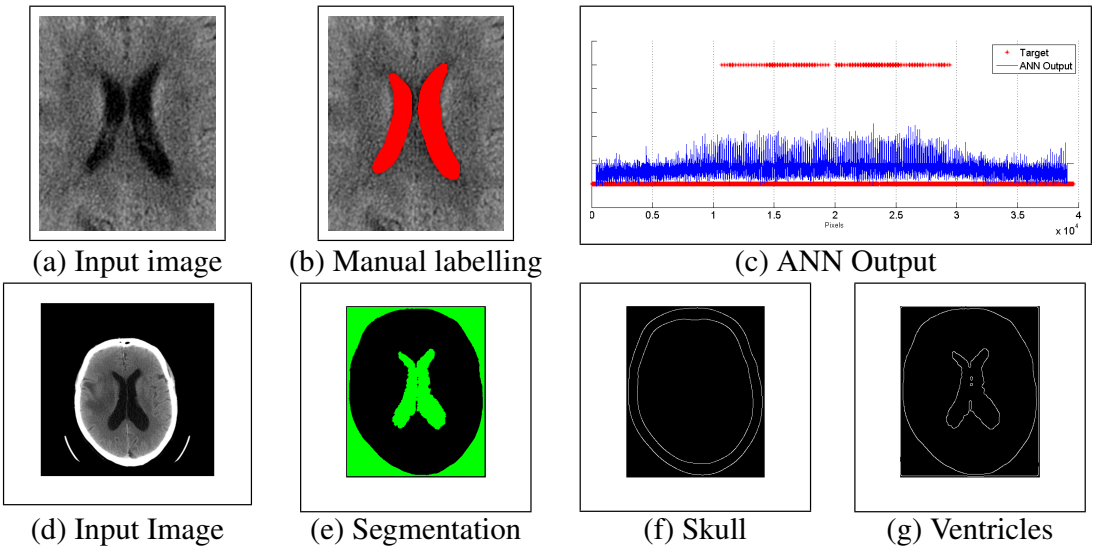

(a) Input image (b) Manual labelling (c) ANN Output

(d) Input Image (e) Segmentation (f) Skull (g) Ventricles

Figure 3: Segmentation of the ROI in Brain CT Scans.

measurement algorithm. An expert then provides multiple reference measurements in an interactive session using a simple user interface and the averages are stored as benchmarks P_{cal} for subsequent automatic measurements. There is an option to use Metric or Imperial units for measurements. The contiguous image regions from step 2.2 are used to determine measurements such as extrema, centroid, area, major and minor axes. The values of extrema are used to draw reference points (Fig. 1a) around the ROI using same approach as section 2.1 and the number of pixels between relevant points is divided by P_{cal} to give measurements. To estimate the indices, the distance between relevant reference points is counted in terms of pixels and appropriate formula is applied from atlas [3].

3 Experimentation Results

The technique has been applied on 48 noncontrast CT studies from different subjects with ages between 5 to 85 years including 14 subjects from the National Cancer Institute public dataset. Two radiology experts independently performed manual segmentation and calculated ratios and indices to be used for training and evaluation in our experiments. The subjects' personal information was anonymized and only age and gender data were retained. Measurements of the maximum frontal horn diameter (A), inner skull diameter at the level of frontal horns (D), maximum inner skull diameter (F), outer skull diameter at the frontal horns (G), maximum outer skull diameter (H) and minimum width of the later ventricles separated by the septum (I) were made by experts. Our method repeated the same linear measurements after segmenting the ROI and using reference points and calibration information. The results were compared with the measures in noncontrast CT scans from different age groups and showed ICC ≥ 0.97. Correction of orientation of head showed 85% sensitivity and 75%, while detection of brain midline shift $> 5mm$ showed sensitivity and specificity of 80% and 86% respectively. The intraclass correlation coefficient (ICC) was calculated using MedCalc to compare the results with experts to ascertain reliability of measurements. Linear measurements show ICC range from 0.97 to 0.99 and the results are given in table 1. For both the CMI and ER estimations, ICC was 0.98 compared to the experts. The optimum testing performance of 88.9% of the ANN was observed with 10 hidden neurons to segment the

Label	Measurement	ICC
A	Maximum frontal horn diameter	0.99
D	Inner skull diameter at the level of the frontal horns	0.97
F	Maximum inner skull diameter	0.97
G	Outer skull diameter at the frontal horns	0.97
H	Maximum outer skull diameter	0.98
I	Minimum width of the lateral ventricles separated by the septum (cella media)	0.98

Table 1: Measurements on the axial CT scans

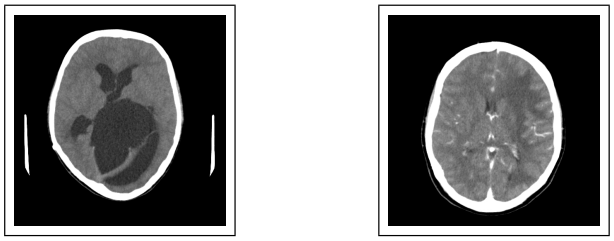

(a) Transtentorial Arachnoid cyst (b) Metastatic lesions

Figure 4: Cases excluded from experiments.

image using 70% training, 15% validation and 15% test samples. Increasing or decreasing the number of hidden neurons in ANN did not significantly improve the performance and the average performance was $87.4-88.9\%$ in training and testing. The sliding window in section 2.2 was evaluated with varying sizes of 3×3, 5×5 and 7×7 neighbourhood pixels, however, the optimum output was achieved with 5×5 pixels windows for extracting features. The experiments were performed using Matlab R2013b on Mac OS X and Windows 7 platforms. The average time taken by our method to perform segmentation and estimations of indices and ratios was ≤ 20 seconds because the algorithm performs the segmentation and measurements in toto without performance degradation. CT studies of patients with gross deformity of the brain structure due to either neoplastic metastasis, pathology or trauma gave less satisfactory estimations and resulting measurements were amiss. These 2 of the 34 cases (fig. 4) were excluded from the performance analyses after preliminary experiments.

4 Conclusion

Manual demarcation of ROI by expert radiologists is still considered gold standard, however, our proposed system has shown plausible results with $87.4-88.9\%$ accuracy with ANN in segmenting the ROI which are used as reference points for estimating various brain indices. The error in linear measurements on noncontrast axial CT scans was less than $\pm1mm$ and ICC results were ≥ 0.97 compared with experts. Correction of orientation of head and detection of midline shift $> 5mm$ showed sensitivity of 85% and 80% and specificity of 75% and 86% respectively. The average time taken for measurements was also significantly reduced. Currently, the CT slice with pertinent anatomical landmarks is manually input to the system for measurements. However, we are working on an algorithm to automatically select the representative slice from the complete study of the subject. Interpretation of the

medical images by the radiologists is fraught with errors and variations which represent the weakest aspect of clinical imaging. Based on the results of our method, we propose that integration of automated systems in clinical and research settings can significantly reduce the radiologists' workload and inter-observer variability in assessing normal development, ageing, pathological and traumatic cases.

References

[1] S. Barker-Collo, M. Kahan, and N. Starkey. Computerised tomography indices of raised intracranial pressure and traumatic brain injury severity in a new zealand sample. *The New Zealand medical journal*, 125(1360):92, 2012.

[2] E. González-Reimers and F. Santolaria-Fernández. Brain atrophy in alcoholics. In *Handbook of Behavior, Food and Nutrition*, pages 2993–3010. Springer, 2011.

[3] T. Keats and C. Sistrom. *Atlas of radiologic measurement*. Mosby Inc, 2001.

[4] T. Kondo and J. Ueno. Feedback GMDH-type neural network and its application to medical image analysis of the liver cancer. In *42th ISCIE international symposium on stochastic systems theory and its applications*, pages 81–82, 2012.

[5] I. Kononenko. Machine learning for medical diagnosis: history, state of the art and perspective. *Artificial Intelligence in medicine*, 23(1):89–109, 2001.

[6] V. Schetinin and J. Schult. A neural-network technique to learn concepts from electroencephalograms. *Theory in Biosciences*, 124(1):41–53, 2005.

[7] V. Schetinin and J. Schult. Learning polynomial networks for classification of clinical electroencephalograms. *Soft Computing*, 10(4):397–403, 2006.

[8] Z. Shi and L. He. Application of neural networks in medical image processing. In *Proceedings of the Second International Symposium on Networking and Network Security*, pages 2–4, 2010.

[9] W. Tao, H. Jin, and Y. Zhang. Color image segmentation based on mean shift and normalized cuts. *Systems, Man, and Cybernetics, Part B: Cybernetics, IEEE Transactions on*, 37(5):1382–1389, 2007.

[10] S. Vantaram and E. Saber. Survey of contemporary trends in color image segmentation. *Journal of Electronic Imaging*, 21(4):040901–1, 2012.

[11] R. Wilk, E. Kluczewska, B. Syc, and G. Bajor. Normative values for selected linear indices of the intracranial fluid spaces based on ct images of the head in children. *Polish Journal of Radiology*, 76(3):16, 2011.

[12] Y. Zhang, E. Londos, L. Minthon, C. Wattmo, H. Liu, P. Aspelin, and L. Wahlund. Usefulness of computed tomography linear measurements in diagnosing alzheimer's disease. *Acta Radiologica*, 49(1):91–97, 2008.

[13] V. Zharkova and V. Schetinin. Filament recognition in solar images with the neural network technique. *Solar Physics*, 228(1-2):137–148, 2005.